Hindawi
Journal of Chemistry
Volume 2020, Article ID 8185037, 12 pages
https://doi.org/10.1155/2020/8185037

Research Article

The Effect of Limited Proteolysis by Trypsin on the Formation of Soy Protein Isolate Nanofibrils

Di An and Liang Li

College of Food Science, Northeast Agricultural University, Harbin 150030, China

Correspondence should be addressed to Liang Li; liliangneau@163.com

Received 18 February 2020; Accepted 9 April 2020; Published 26 April 2020

Academic Editor: Zoran Vujcic

Nanofibril system constructed by protein self-assembly is widely used in the food industry because of purposive functional properties. Soy protein isolate nanofibrils (SPINs) were reported to form via heating at pH 2.0. In this research, the soy protein isolate (SPI) hydrolysate prepared by trypsin was used as a raw material for the formation of nanofibrils called soy protein isolate hydrolysate nanofibrils (SPIHNs). Microscopic images demonstrated the formation of two nanofibrils. Based on circular dichroism spectroscopy and Thioflavin T (ThT) fluorescence spectral, we concluded that β-sheet played an important role in SPIN and SPIHN's structural composition. At the same time, the α-helix in SPI had not been destroyed, thereby favoring the formation of SPIHN. The surface hydrophobicity of SPIHN continued to increase during the heating process and reached the highest value when heating 8 h. SDS-PAGE analysis showed that peptides produced by enzyme-modified SPI affected the formation of SPIHN. These results proposed that enzymatic hydrolysis prior to acidic during fibrillation process affected the fibrillation of SPI, and the peptides formed by enzymatic hydrolysis were more efficient for the self-assembly process. This study will provide a theoretical basis for the future research of SPI nanofibril functionality.

1. Introduction

Self-assembly has been applied as an emerging method for the study of functional properties of proteins. In past studies, many proteins including egg protein [1], whey protein [2, 3], soy protein [4, 5], and bovine serum albumin [6] had been confirmed to form nanofibrils by self-assembly under acidic conditions (pH 2.0), accompanying the heating process. The nanofibrils are morphologically characterized by a linear fibril structure with a nanometer diameter and a micron length [7]. In general, it has been confirmed that nanofibril generation mainly depended on the interaction of noncovalent bonds, which is the synergistic result of hydrogen bonding, hydrophobic interaction, and electrostatic interaction [7]. Since cysteine residues were protonated during fibrillation, disulfide bonds do not play an important role in fabrication and stabilization of nanofibrils [8]. At the same time, a significant structural change occurs in the self-assembly of proteins and cross-repetitive β-sheet structure provides a unique structure [9]. In food science, researchers focus on wide applications of protein fibrillation such as functional enhancement [10]. The nanofibrils present diverse and reactive functional groups on their surface, which makes them tunable by numerous agents.

Peptides are widely accepted as the building blocks of heat-induced nanofibrils [11]. Hydrolysis occurs before aggregation, and different peptides have a significant effect on the structure of aggregates [12]. Therefore, prehydrolyzed proteins rather than intact proteins have accordingly been utilized for fabrication of the nanofibrils. More importantly, the hydrolysis kinetics affect the growth kinetics of nanofibrils the same as temperature, concentration, and time [13]. So enzymatic hydrolysis of proteins could participate in the fibrillation process of nanofibrils and played a role in the growth of nanofibrils.

SPI is a mixture of several proteins that are widely used in industrial production because of their good functional properties, and it plays an important role in plant protein resources. Slender, semiflexible nanofibrils were formed from SPI when heated at 85°C and pH 2.0 [5]. Akkermans et al. found that most properties of soy protein nanofibrils were comparable to whey protein and even better than whey

protein in some respects [5]. Long-term research showed that soy protein could be fabricated into various nanostructures. Therefore, nanofibrils which are based on soy protein have widespread application prospects. Enzymatic hydrolysis had been successfully applied to soy protein isolates to produce functional peptides [14]. Enzymatic hydrolysis produces peptides that may provide a new self-assembly strategy for nanofibrils prior to acid hydrolysis. The combination of enzymatic hydrolysis and self-assembly can improve the functional properties of proteins [15]. This study aimed at the hydrolysis of SPI by trypsin and then induced the hydrolysis products to form nanofibrils, comparing the morphological, structural, and functional properties of the SPIHN with SPIN. The objectives of this work were to study the importance of enzymatic hydrolysis in the formation of nanofibrils. The results would reveal the mechanism of enzymatic hydrolysis on the self-assembly process and found new ways to produce nanofibrils.

2. Materials and Methods

2.1. Materials. SPI was purchased from Harbin High-Tech Co., Ltd. (Harbin, China). The basic composition and content of SPI are shown in Table 1. Trypsin (with a minimum activity of 250 NFU·mg^{-1}), papain (with a minimum activity of 8×10^5 U·g^{-1}), and neutral protease (with a minimum activity of 5×10^4 U·g^{-1}) was obtained from Solarbio (Shanghai, China). Bicinchoninic acid (BCA) protein assay kit was purchased from Nanjing Jiancheng Biotechnology Institute Co., Ltd.(Nanjing, China). O-Phthalaldehyde (OPA), 1,4-dithio-DL-threitol (DTT), sodium dodecyl sulfate (SDS), and gel electrophoresis-related reagents were obtained from Solarbio (Shanghai, China). 2-[4-(Dimethylamino)phenyl]-3,6-dimethylbenzothiazolium chloride (Thioflavin T, ThT) was purchased from Yuanye (Shanghai, China). Anilinonaphthalene-8-sulfonate (ANS) was obtained from Aladdin (Shanghai, China). Other undescribed chemical reagents were of analytical grade.

2.2. Nanofibril Formation. SPI was dissolved in 50 mL distilled water at 4% (W/V). The solution was stirred at room temperature and stored at 4°C overnight for full hydration. Three enzymes were added to the solutions, and then the solutions were adjusted to the appropriate reaction conditions of the three enzymes. The fibrillation process followed the method reported by Tang et al. [16]. Next, the hydrolysates were adjusted to pH 2.0 using 6 M HCl and heating at 85°C for fibrillation. In order to terminate the reaction, the heated sample was placed in an ice bath and the sample was preserved at 4°C.

2.3. Degree of Hydrolysis (DH). The DH measurement by the OPA method as reported by Nissen [17]. The 100 mL OPA solution was as follows: 3.81 g sodium tetraborate, 100 mg sodium dodecyl sulfate (SDS), 80 mg OPA (dissolved in 2 mL of anhydrous ethanol), and 88 mg DL-dithiothreitol. 400 μL SPI hydrolysate (100-fold dilution) was added to 3 mL OPA solution and reacted in the dark for 2 min. The absorbance was measured at 340 nm by a UV-visible spectrophotometer (UV2600, Shimadzu, Japan). The results were calculated using a standard curve prepared with serine. The DH was calculated using the following equation:

$$\mathrm{DH} = \frac{h_1 - h_0}{h_{\mathrm{tot}} - h_0} \times 100\%, \quad (1)$$

where h_1 and h_0 represent the amino acid concentrations of hydrolyzed and nonhydrolyzed SPI, respectively. h_{tot} is the total amino acid concentration of SPI.

Table 1: Basic composition and content in SPI.

Components	Protein	Crude fat	Moisture	Ash
Contents	91.32 ± 0.78	1.62 ± 0.42	3.52 ± 0.56	3.54 ± 0.85

2.4. Atomic Force Microscope (AFM). The microstructure images were analyzed by AFM. The samples were diluted to 0.01 mg·mL^{-1} with distilled water (pH 2.0). Then, 20 μL diluted sample was added to a glass slide and air-dried for 30 min at room temperature. Imaging was performed by Icon (Dimension Icon, Bruker Ltd., US) in the tapping mode, and the scan rate was 1.2 Hz. AFM images were processed by NanoScope Analysis (1.8.0.0).

2.5. Particle Size Measurement. Particle size distribution and light scattering intensity of nanofibrils were measured by Zetasizer Nano (Zetasizer Nano Zs, Malvern Instruments Ltd., UK). The samples' concentration was diluted to 0.1 mg/mL with distilled water (pH 2.0). The distilled water was filtered by a 0.22 μm filter before being used. The diluted sample was added into the cuvette, and the sample amount according to the reference quantity was provided by the instrument manufacturer. Dynamic light scattering (DLS) analysis was performed with a backscattering angle of 173° and a refractive index of 1.45 for protein particles at 25°C.

2.6. Sodium Dodecyl Sulfate Polyacrylamide Gel Electrophoresis (SDS-PAGE). SDS-PAGE in a discontinuous vertical plate system according to Laemmli's method [18]. The gel sheet used in the experiment was 10% resolving gel (pH 8.8) and 5% stacking gel (pH 6.8). The sample was diluted to 2 mg/mL by dilution. The diluted sample was heated in a water bath at 100°C for 4 min, cooled, and centrifuged at 11000 ×g for 5 min. Marker's molecular weight range was from 11 kDa to 180 kDa. 10 μL of sample supernatant and 5 μL of marker were loaded into the lanes. The gel was stained with Coomassie brilliant blue G250 for 30 min, and the gel sheet was then decolorized.

2.7. Determination of Surface Hydrophobicity. Using ANS to measure surface hydrophobicity is the most appropriate method for analyzing the three-dimensional structure of proteins [19]. According to the method of Luo et al. and modifying it [20], the samples were diluted to 0.02, 0.04, 0.08, and 0.16 mg/mL with 0.01 mol/L phosphate buffer (pH 7.0). Then, 30 μL ANS solution (8 mmol/L ANS and

0.01 mol/L phosphate buffer at pH 7.0) was added to aliquots of the dilute sample (5 mL), and the mixture was vortexed and reacted in dark for 15 min. The fluorescence spectra were obtained by a fluorescence spectrometer (Hitachi F4500, Hitachi High-Technologies Corp., Japan). The parameter excitation wavelength was 390 nm, emission wavelength was 400–600 nm, and slit width was 10 nm. The initial slope of the regression line in the curve of protein concentration and fluorescence intensity is the surface hydrophobicity of the protein.

2.8. ThT Fluorescence Assay. The stock solution (0.8 mg/mL ThT, 10 mM phosphate, and 150 mM NaCl, pH 7.0) was filtered through a 0.22 μm filter. ThT stock solution was sealed with metal foil and stored in the refrigerator at 4°C. The working solution was prepared by diluting the ThT stock solution 50-fold with the above phosphate-NaCl buffer. 50 μL sample was mixed with 5 mL ThT working solution, and the mixture was magnetic stirred for 1 min. The fluorescence intensity was obtained by a fluorescence spectrometer (Hitachi F4500, Hitachi High-Technologies Corp., Tokyo, Japan). The excitation wavelength was 460 nm (slit width = 5 nm), and the emission spectra were obtained from 480 to 550 nm with a scanning speed of 240 nm/min.

2.9. Circular Dichroism Spectroscopy. Circular dichroism spectroscopy (CD) can analyze changes in secondary structure of SPIN and SPIHN. Far-UV region (190–260 nm) spectra were measured at room temperature with Jasco spectropolarimeter (model J-815, Jasco, Japan). Different samples were diluted to 0.2 mg/L by distilled water, and the samples were placed in a 1.0 mm path length quartz cells and scanned at 100 nm/min. All data were analyzed by CDNN software.

2.10. Statistical Analysis. All experiences were analyzed in triplicate, and values given in the tables and figures were reported as the mean ± standard deviation (error bars). Statistical analysis was performed using the SPSS (20.0) software. Significance of differences ($p < 0.05$) between means was determined by Duncan's multiple-range test.

3. Results and Discussion

3.1. Selection of Enzymes and Determination of Degree of Hydrolysis. Three common enzymes, including trypsin, papain, and neutral proteases, were selected in this study. Excessive hydrolysis will greatly reduce the production of nanofibril because the nonnucleated regions will be separated from the self-assembled regions of the nanofibril, thus affecting the nanofibril formation process [21], and the degree of hydrolysis of enzyme-modified soy protein was usually controlled between 1% and 25% [22]. According to our research requirement, we controlled the same hydrolysis degree (1%) of three SPI enzymatic hydrolysate (trypsin, 18 min; papain, 5 min; neutral protease 9 min; Figure 1). The three hydrolysates of SPI were formed to nanofibrils via heating at pH 2.0 with different times (1, 2, and 4 h). According to the ThT fluorescence intensity analysis (Figure 2), it could be concluded that the fluorescence intensity of the trypsin group increased significantly with time, while the fluorescence intensity of the papain and neutral protease groups did not change substantially and the peak values were low. This indicated that less nanofibrils were formed by the papain and neutral protease treatment. The nucleation mechanism indicated that homogeneous nucleation was essential for the fibrillation process, and the wrong nucleation process will lead to the emergence of nonfibril aggregates [23].

3.2. Atomic Force Microscope (AFM) Analysis. AFM as one of the most versatile single-molecule techniques has emerged within the last decade as a powerful tool for the study of the structural properties of nanofibril and the fibrillation process [24, 25]. Figure 3 shows the AFM images of SPIN and SPIHN. When unheated, there was no large aggregates in the SPI, and protein exhibited the spherical structure. We tried to study the formation of two kinds of nanofibrils by prolonging the heating time. When heated for 8 h, there was a significant difference in the AFM images of the two nanofibrils. In SPIN (Figure 3(b)), the morphology of the nanofibrils was short and thick with an average length of 302 nm. In SPIHN (Figure 3(c)), nanofibrils with an average length of 194 nm were shorter than SPIN, had almost no branches, and appeared more flexible in morphology. This indicated that enzymatic hydrolysis played a role in the formation mechanism of nanofibrils, which changed the morphology of nanofibrils. Fibril-forming peptides prepared by enzymatic hydrolysis could result in minor differences in binding between peptide units, which were infinitely magnified during nanofibril development, and could lead to morphological differences [26]. Many nonfibril aggregates were observed in SPIN; instead, there was no appearance of aggregates in SPIHN. The appearance of aggregates may indicate that the fibrillation process had entered the later stage, that is, the reverse phase of nanofibril formation, and the nanofibrils were decomposed into different monomers. Whereafter, a portion of the unstable monomers converge to form nonlinear aggregates with different sizes and morphologies [27]. Generally, the nanofibrils entangled and clustered at some domains [2]. But the domains could clearly observe the fibril-like structure, while the aggregates in SPIN appeared as dense spheres. We believed that the formation of aggregates was due to unstable monomers.

It is clear that the unfolding of proteins is a common requirement before self-assembly forms nanofibrils [28]. The conformationally altered monomer or the partially unfolded state has a strong tendency to form protein nanofibrils. Formation of protein aggregates with random shape during the enzymatic hydrolysis of proteins could probably influence the fibrillation extent [29].

3.3. Particle Size Measurement. DLS was very sensitive to the formation of tiny aggregates in protein solutions [30]. Once the monomer particles in the solution were aggregated, the light waves will change greatly.

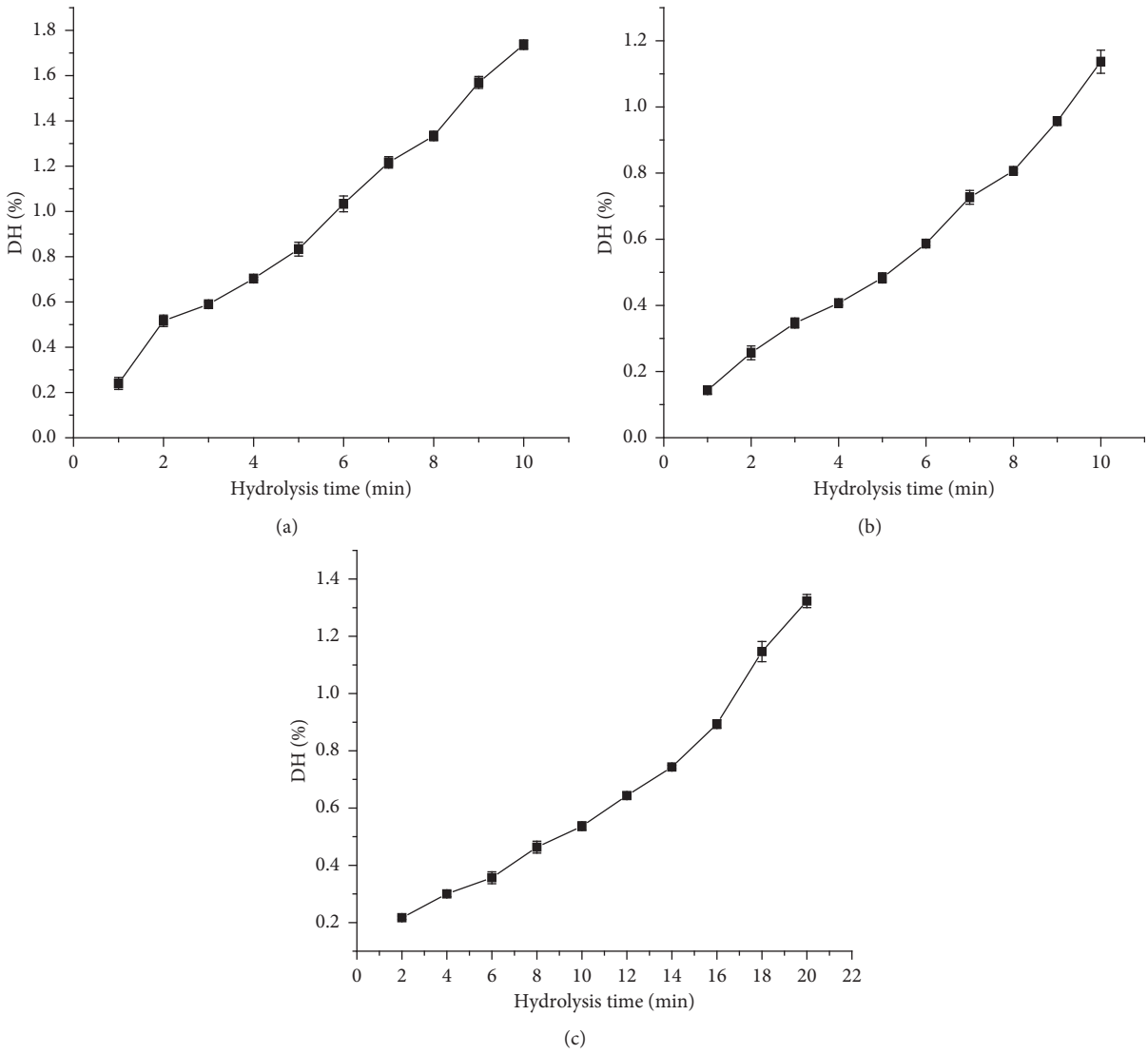

Figure 1: The effect of time on the degree of hydrolysis of SPI: (a) papain; (b) neutral protease; (c) trypsin.

Figure 4 shows that particle size distribution of samples with different heating times. Figure 4(a) shows that SPIN had a small change in particle size distribution between 0 h and 2 h, which may be the preparation stage for fiber formation. Bimodal peaking began to appear when heated for 4 h, four peaks appeared when heated for 8 h, and the peak value of the aggregate had reached 1000 nm. Figure 4(b) shows that the peak of the particle size distribution of SPIHN did not change from 0 h to 2 h, which was consistent with SPIN. When heated for 4 h, the bimodal contribution indicated that the formation of nanofibrils (especially elongation of nanofibrils) was only formed during heating with enough time [31].

Figure 5 shows the average particle size change in SPIN and SPIHN. Enzymatic hydrolysis reduced the average particle size of SPI. The average particle size of SPIN was decreasing from 0 h to 2 h. The phenomenon of SPIHN occurred from 0 h to 4 h. This should be because heating caused the protein to release more peptides, which was known as the preparation phase of the fibrillation process [32]. Akkermans et al. demonstrated the self-assembly fibrillation process was related to the changes in protein conformation and peptide hydrolysis, and peptides were the main building blocks of self-assembly fibrils [11]. The change in the average particle size indicated that the enzymatic hydrolysis did not significantly affect the minimum average particle size, which was consistent with the results of Xia et al [33]. We found a more interesting phenomenon; that is, the minimum average particle size of nanofibrils was between 100 nm and 150 nm. We could boldly guess that the particle size of the system after releasing the peptide also affects the self-assembly process. After heating for 4 h, the average particle size of SPIN and SPIHN increased rapidly. Peptides with excellent self-assembly ability as building blocks rapidly

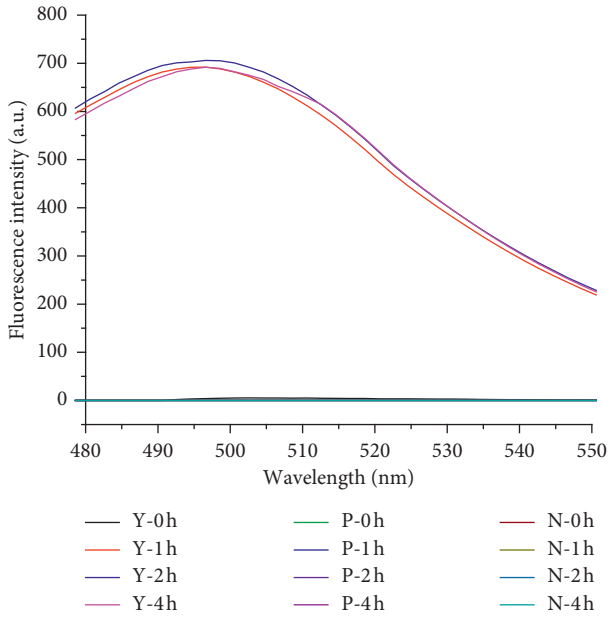

Figure 2: ThT spectroscopic profiles of nanofibers. Y: trypsin; P: papain; N: neutral protease.

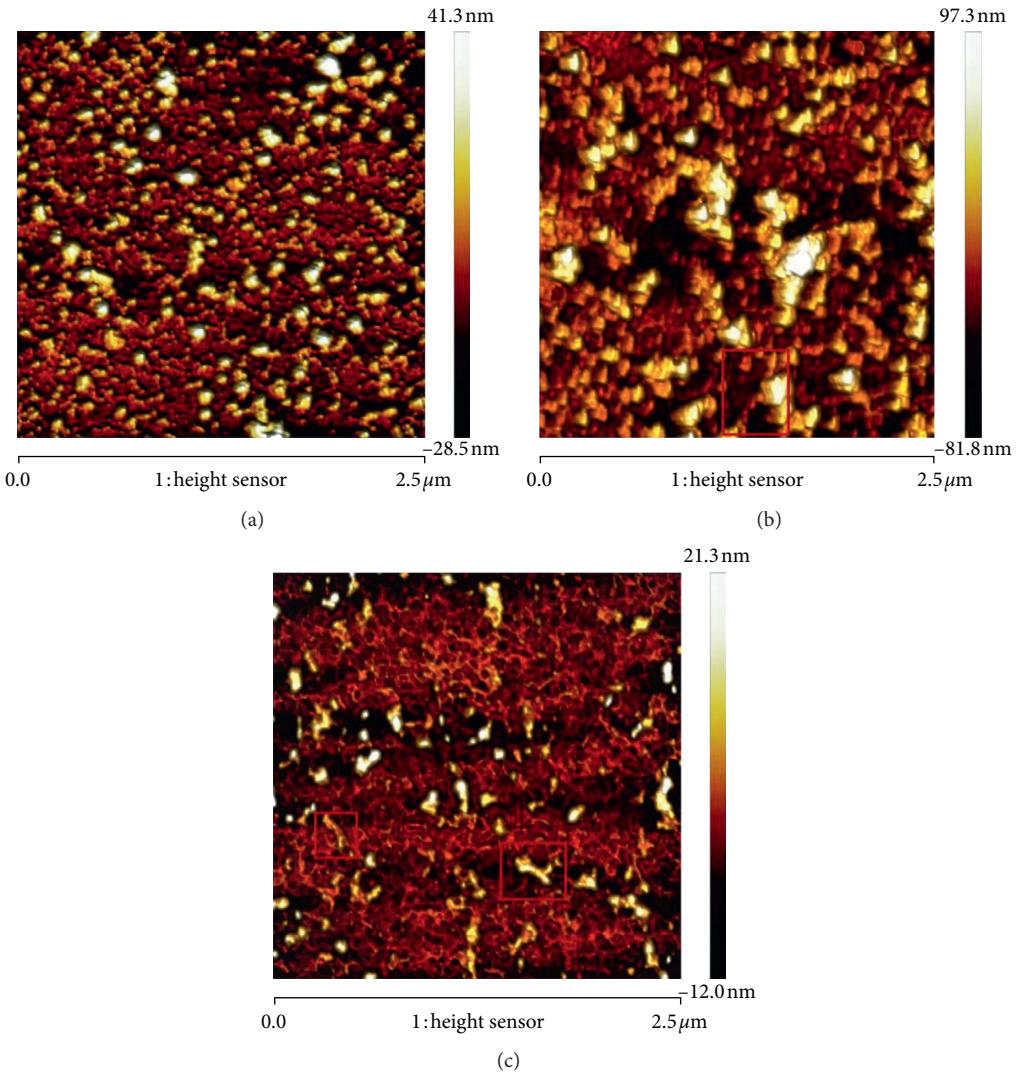

Figure 3: AFM micrographs of nanofibrils in SPI solution: (a) SPI, 0 h; (b) SPIN, 8 h; (c) SPIHN, 8 h.

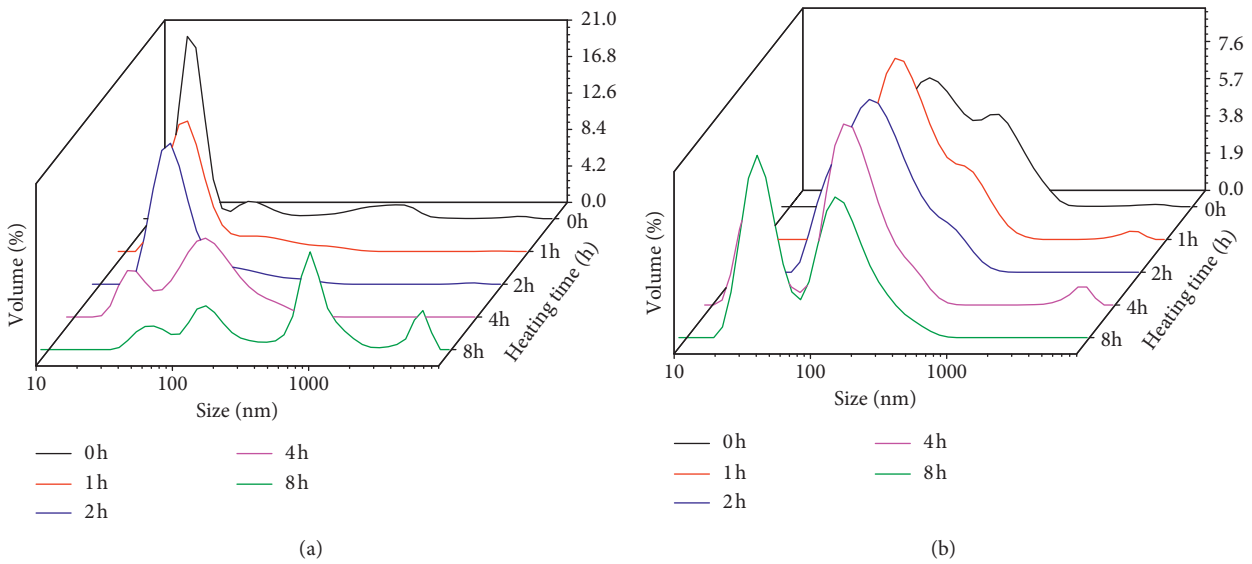

Figure 4: Particle size profiles of SPIN (a) and SPIHN (b).

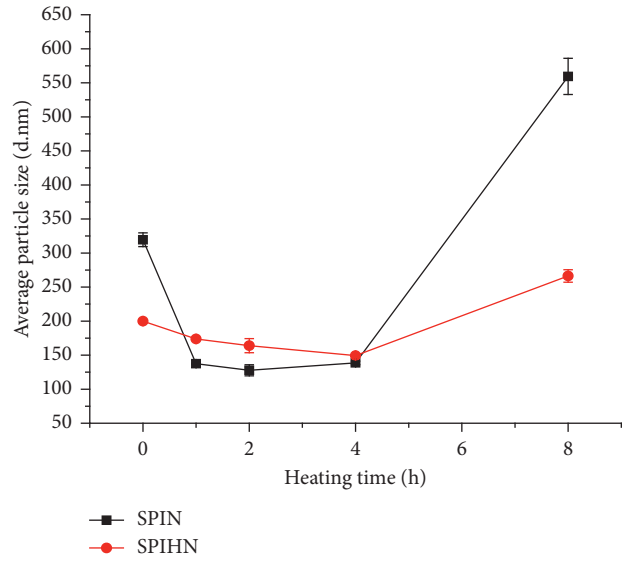

Figure 5: The average particle size profiles of SPIN and SPIHN.

form nanofibrils. When heated for 8 h, the average particle size of SPIHN and SPIN reaches 559.37 ± 26.58 nm and 255.77 ± 9.24 nm.

3.4. ThT Fluorescence Assay. ThT is cationic benzothiazoles that combine with the β-sheet structure of nanofibrils to increase the fluorescence intensity significantly [34]. The possible mechanism was that the thiazole nitrogen forms a hydrogen bond with the hydroxyl group of the tissue structure, allowing these dye molecules to specifically bind to the nanofibrils [35]. Vassar demonstrated that ThT bonded to nanofibrils better than congo red, crystal violet and Van Gieson [36]. ThT could be used as a fluorescent indicator, which detected the dynamic process of nanofibril formation [37].

Prior to heating, the natural and hydrolyzed SPI fluorescence intensity curves did not change (Figure 6(a)). This was because they contain highly twisted β-sheets structure, but few β-strands cause the binding sites to be short or distorted, resulting in failure to combine with ThT [38, 39]. When the heating time was continuously increased, the fluorescence intensity of SPIN and SPIHN was significantly increased because the β-sheets structure gave rise to a specific sequence of cross-strand ladders during self-assembly, and these specific side chains could allow ThT to bind [40]. The fluorescence intensity of untreated SPI-forming nanofibrils was much lower than the nanofibrils previously reported by Tang et al. because the affinity of ThT was lower at acidic conditions than at neutral conditions, and this was because the electrostatic repulsion of positive charges hindered the combination of dyes and nanofibrils [41]. However, increasing the ionic strength could shield the charges between dye and nanofibrils to overcome the decrease in affinity at acidic pH [42], but in order to discuss the effect of enzymatic hydrolysis on the formation of nanofibrils, this study did not add salt in system. The fluorescence intensity of SPIN decreased when heating time from 4 h to 8 h. At this time, the average particle size of SPIN reached the maximum value, and the decreased fluorescence intensity may be attributed to the disordered aggregation of nanofibrils into other nanofibrils [43, 44], but not all nanofibrils had been transformed, so the fluorescence intensity was not rapidly decreased. The fluorescence intensity of SPIHN reached the maximum at 8 h, which was 2179.46 ± 12.56.

It could be seen from Figure 6(c) that there was no significant difference in the maximum fluorescence intensity of SPIHN when heated for 1 h–4 h, indicating that a large number of nanofibrils were not generated. The maximum fluorescence intensity of SPIN had a significant difference. The process of nanofibrils formation went through the nucleation period [45]. Maximum fluorescence intensity indicated that SPIN generated faster than SPIHN, and

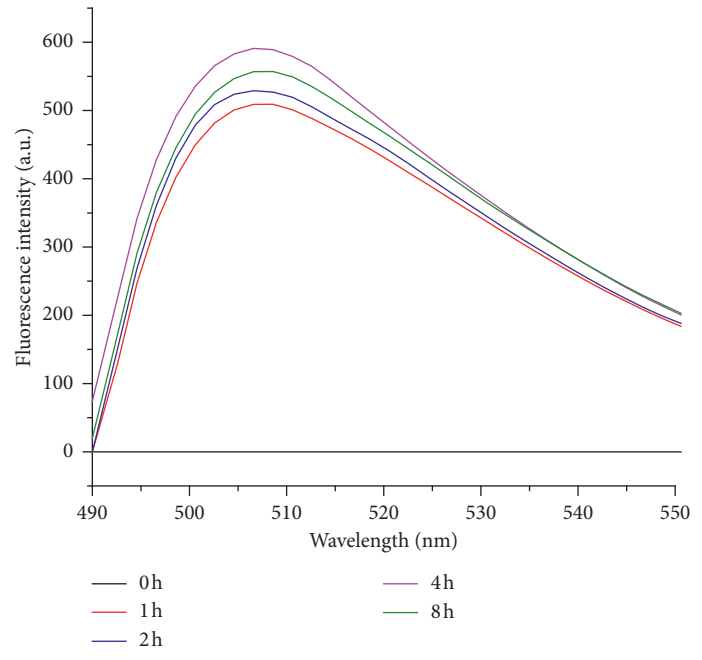

(a)

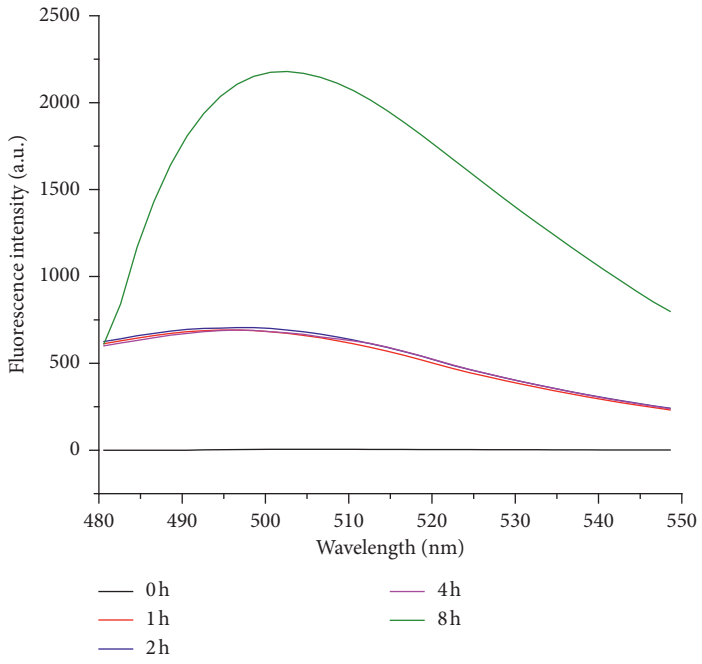

(b)

Figure 6: Continued.

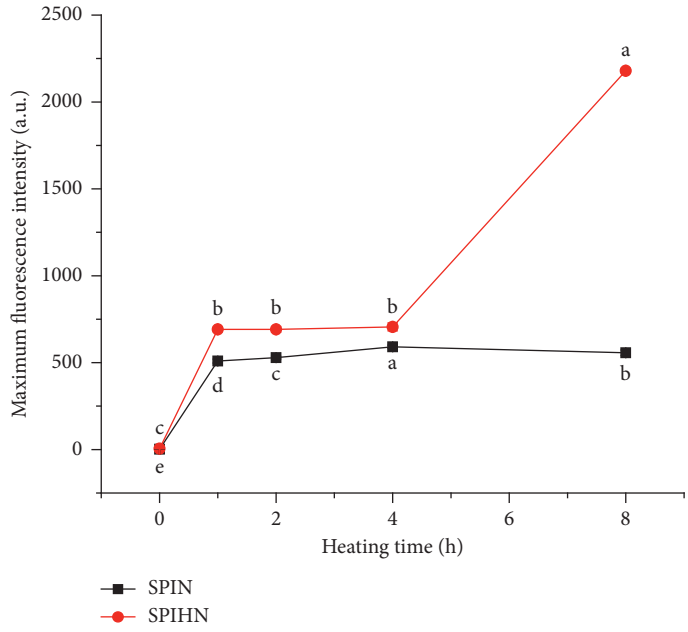

(c)

Figure 6: ThT spectroscopic profiles of SPIN and SPIHN.

SPIHN required longer nucleation time than SPIN. The theory of self-assembly mechanism established by Mishra et al. indicated that nicking will form during the protein self-assembly fibrillation process. When proteins lost peptides, the nicking was formed. These proteins will form the core of nanofibrils [46]. Enzymatic hydrolysis greatly increased the number of peptides resulting in nicking. Therefore, SPIHN had a longer nucleation time, and the maximum fluorescence intensity was significantly increased after heating for 8 h.

Table 2: The surface hydrophobicity of SPIN and SPIHN.

Heating time (h)	SPIN	SPIHN
0	865.16 ± 4.90a	1394.74 ± 7.40d
1	116.01 ± 0.39c	1778.33 ± 34.95c
2	128.88 ± 0.71b	1783.53 ± 40.36c
4	107.48 ± 0.89d	1885.33 ± 7.51b
8	91.55 ± 1.17d	2003.84 ± 8.17a

Different letters in the same column indicate significant differences ($p < 0.05$).

3.5. Surface Hydrophobicity Determination. Surface hydrophobicity can reflect the number of hydrophobic groups on the surface of protein molecules and also reflects change in the molecular structure of proteins [47]. The change in surface hydrophobicity can well reflect the effect of hydrophobic interaction on the formation of protein aggregates [48]. Table 2 shows the surface hydrophobicity of SPIN and SPIHN at pH 2.0 for different heating times (0, 1, 2, 4, and 8 h). The surface hydrophobicity of untreated SPI was 865.16 ± 4.90. When heating began, the surface hydrophobicity of SPIN decreased drastically. The previously described nicking theory could explain this phenomenon, and the special region of nicking with high hydrophobicity and low charge will form the core of nanofibrils [46]. Nucleation process resulted in aggregation of hydrophobic groups exposed to heat. In the initial stage of heating (from 1 h to 2 h), the surface hydrophobicity had a significant increase. Nanofibril formation process leaded to peptides with a higher surface hydrophobicity self-assembled to fibrillar structures during the heating at pH 2.0 [49]. When heated for 4 h, the surface hydrophobicity had a significant decrease. After reaching a maximum, the surface hydrophobicity of SPIN tended to decrease because of aggregation, during which the exposed hydrophobic groups were buried in the nanofibrils [50].

In SPIHN, the surface hydrophobicity of SPI modified by trypsin significantly increased. Trypsin-modified SPI will produce hydrophobic amino acids, such as arginine and lysine [51]. The surface hydrophobicity of SPIHN continued to increase at different heating times, which was much greater than SPIN. The result of SPIHN was consistent with that reported by Gao et al [8], and Gao found that nanofibrils formed by the four enzyme-modified proteins all showed an increase in surface hydrophobicity. Partial unfolding of proteins during fibrillation will expose more hydrophobic groups, which may promote the formation of nanofibril. In addition, surface hydrophobicity was a structure-related function, depending on the size and shape of protein molecule, amino acid composition, and sequence, as well as any intramolecular or intermolecular cross-links [52, 53]. Therefore, it was necessary to choose more reasonable means to modify the protein and improve the surface hydrophobicity. Xu et al. reported that the surface hydrophobicity of the high concentration SPI had a high value during heating,

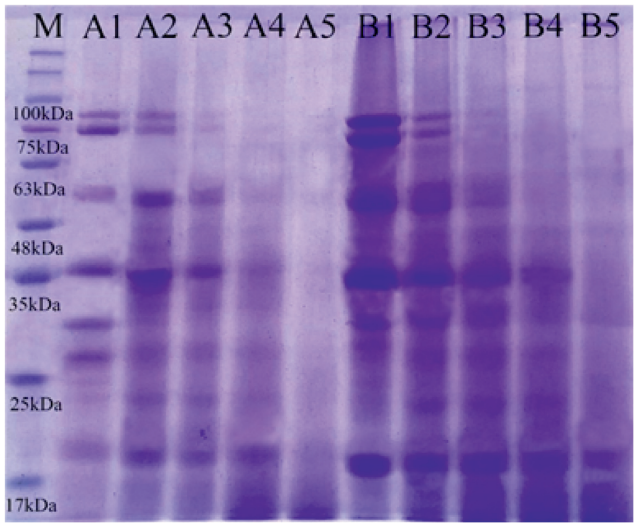

Figure 7: SDS-PAGE patterns of different samples (SPINA1–A5 (0, 1, 2, 4, and 8 h); SPIHNB1–B5 (0, 1, 2, 4, and 8 h)).

indicating the effect of concentration on the surface hydrophobicity of the protein during heating [32]. Changing protein concentration was probably the easiest way.

3.6. Sodium Dodecyl Sulfate Polyacrylamide Gel Electrophoresis (SDS-PAGE) Analysis. Figure 7 shows SDS-PAGE images of SPIN and SPIHN. Untreated SPI and trypsin-modified SPI have two high-molecular-weight major bands (86 kDa and 74 kDa). As the heating time increased, both of the main bands disappeared. After heating for 2 h, neither of SPIN nor SPIHN observed these two bands. In addition to the two major bands, many low-molecular-weight bands had emerged, which might be peptide fragments released by heating at acidic pH. There were persistent bands of between 25 and 63 kDa that remained dominant at 1, 2, and 4 h. When heated to 8 h, there were almost no bands in the lane A5, the molecular weight was concentrated at 19 kDa in the lane B5, and a part of the molecular weight was <17 kDa. SPIHN had stronger bands than SPIN at 19 kDa at different times, which indicated that the prehydrolyzed sample was heated at acidic conditions producing a heterogeneous mixture of the peptides affecting the formation of SPIHN. The AFM image showed that SPIHN had better fibrillation outcome than SPIN when heated for 8 h. Combined with electrophoresis bands, we concluded that the low-molecular-weight peptide (about 19 kDa) assisted SPIHN with formation of more nanofibrils. The low-molecular-weight peptide produced by enzymatic hydrolysis provided many building blocks for the formation of nanofibrils. Mohammadian et al. reported that the heterogeneous compounds formed by prehydrolysis affected the self-assembly process of WPI nanofibrils [15]. ThT fluorescence spectroscopy showed that the fluorescence intensity of SPIHN from 0 h to 4 h did not increase significantly compared with SPIN, which may be related to the formation of heterogeneous compounds. The surge at fluorescence intensity of SPIHN at 8 h may indicate that the peptide produced by enzymatic hydrolysis self-assembled to form more nanofibrils.

According to some reports, after long heating of β-lactoglobulin and pea protein, the protein was completely hydrolyzed into peptides smaller than 20 kDa, and no new bands appeared, which was consistent with the results of our study [31, 54]. The process of self-assembly of different proteins continuously generated low molecular peptides. These results may indicate that self-assembly was the process of transferring macromolecular proteins to small molecular peptides.

3.7. Circular Dichroism (CD) Spectroscopy Analysis. The formation of protein nanofibrils is accompanied by changes in the secondary structure, and we can better understand the self-assembly process according to the changes in the secondary structure. When not heated, the α-helix and β-sheet contents of SPI were $16.37 \pm 0.55\%$ and $31.70 \pm 0.44\%$, respectively. When heated for 1, 2, and 4 h, the α-helix of SPIN gradually decreased, while the β-sheet increased continuously (Tables 3 and 4). This indicated that changes in secondary structure were very important for the formation of nanofibrils. Tang et al. demonstrated that the linear aggregates formed by the soy protein self-assembly process were accompanied by the destruction and reorganization of the secondary structure [16], which was consistent with the results of our study. This was because the α-helix was converted to the β-chains, and then, the structural basis was increased for the formation of nanofibrils [55]. Fandrich et al. found that the molecular structure within the nanofibrils was different from the β-sheet in the native proteins [56]. When heated for 8 h, the β-sheet structure, which was one of the indexes for evaluating the formation of nanofibrils [34], decreased to $22.23 \pm 0.12\%$, and the β-turn increased to $24.13 \pm 0.21\%$. The previous analysis indicated that the nanofibrils had entered the reverse reaction phase after heating for 8 h. Aggregation resulted in the destruction of the β-sheet structure of the nanofibril.

Enzymatic hydrolysis affected the secondary structure of SPI, resulting in the decrease in α-helix (7.23% vs. 16.37%) and the increase in β-sheet (41.60% vs. 31.70%). In SPIHN, the β-sheet continued to increase and reached $62.13 \pm 0.15\%$ after heating for 8 h. With the increase in heating time, the content of β-sheet structure in SPIHN increased significantly, which was consistent with the surface hydrophobicity variation trend. The β-sheet formation occurred concurrently with the formation of aggregates with hydrophobic domains [57]. We were not talking too much about the dominance of β-sheets in nanofibrils. Because we found an interesting phenomenon, enzymatic hydrolysis did not lead to the destruction of the α-helix structure in SPIHN, which provided a good basis for the formation of nanofibrils. Gao et al. found the same conclusion with the nanofibrils formed by WPC [8]. The α-helix was used as components of coiled coils, which is the basic folding pattern found in native proteins [58]. It was found that the structural sequence that forms the α-helix requires the participation of hydrophobic residues and polar residues [59]. Dipeptides kinetic studies

Table 3: The secondary structure compositions of SPIN.

SPIN (h)	α-Helix	β-Sheet	β-Turn	Random coil
0	16.37 ± 0.55a	31.70 ± 0.44c	20.60 ± 0.10b	31.33 ± 0.57c
1	9.37 ± 0.35c	38.70 ± 0.26b	9.13 ± 0.25c	42.80 ± 0.46ab
2	6.10 ± 0.30d	43.8 ± 0.35ab	8.67 ± 0.21c	41.40 ± 0.46ab
4	4.20 ± 0.20e	47.27 ± 0.35a	2.50 ± 0.20d	46.03 ± 0.15a
8	11.07 ± 0.05b	22.23 ± 0.12d	24.13 ± 0.21a	42.57 ± 0.15c

Table 4: The secondary structure compositions of SPIHN.

SPIHN (h)	α-Helix	β-Sheet	β-Turn	Random coil
0	7.23 ± 0.06a	41.60 ± 0.17a	4.73 ± 0.21a	46.43 ± 0.40a
1	10.07 ± 0.06a	46.45 ± 0.25b	0.73 ± 0.06b	42.74 ± 0.31a
2	9.10 ± 0.10a	47.7 ± 0.17c	0.67 ± 0.06b	42.37 ± 0.12a
4	10.80 ± 0.10a	51.06 ± 0.21d	0.00 ± 0.00c	38.13 ± 0.21a
8	12.07 ± 0.061a	62.13 ± 0.15e	0.00 ± 0.00c	25.80 ± 0.20b

Different letters in the same column indicate significant differences ($p < 0.05$).

had found that peptide bonds with C-Asp terminal residues exhibited instability under thermal and acid conditions [60]. The appearance of peptides with *N*-terminal-Asp was confirmed by hydrolysis of proteins [29, 61]. Trypsin cleaves the carboxyl sides of the lysine and arginine residues in the polypeptide chain. Aspartic acid, arginine, and lysine are all polar amino acids. More polar amino acids could increase the content of α-helix structure.

4. Conclusion

Hydrolysates produced by papain and neutral protease modification of SPI could not be heated to form nanofibrils at pH 2.0. The nanofibrils formation of SPI and SPI enzymatic hydrolysate were multistage under heating at pH 2.0. SPIHN fibrillated to a more extent and had a more flexible structure. Enzymatic hydrolysis provided more building blocks for the formation of nanofibrils, which improved the properties of nanofibers. In addition, the particle size distribution, ThT fluorescence spectrum, and surface hydrophobicity reflected the dynamic process of self-assembly, and SPIN entered the reverse reaction stage earlier. The formation of SPIN and SPIHN was a process that breaks down high-molecular-weight proteins into low-molecular-weight peptides. The α-helix of the trypsin-modified SPI was not destroyed, which provided a structural basis for the better formation of nanofibrils. This study showed that SPIHN formed by trypsin modification could be readily applied to the food industry, and the next research will focus on the preparation of hydrogels using SPIHN as a delivery system.

Data Availability

The data used to support the findings of this study are included within the article.

Conflicts of Interest

The authors declare that there are no conflicts of interest.

Acknowledgments

This study was supported by the National Key Research and Development Program of China (no. 2018YFD0400500 and 2018YFD0400503) and "Academic backbone" Project of Northeast Agricultural University (no. 18XG28).

References

[1] C. Veerman, G. D. Schiffart, L. Sagis, M. C., and E. van der Linden, "Irreversible self-assembly of ovalbumin into fibrils and the resulting network rheology," *International Journal of Biological Macromolecules*, vol. 33, no. 1–3, pp. 121–127, 2003.

[2] S. M. Loveday, J. Su, M. A. Rao, S. G. Anema, and H. Singh, "Whey protein nanofibrils: the environment-morphology-functionality relationship in lyophilization, rehydration, and seeding," *Journal of Agricultural and Food Chemistry*, vol. 60, no. 20, pp. 5229–5236, 2012.

[3] S. Roshanghias and A. Madadlou, "Functional and gel properties of whey protein nanofibrils as influenced by partial substitution with cellulose nanocrystal and alginate," *International Dairy Journal*, vol. 81, pp. 53–61, 2018.

[4] C.-H. Tang, S.-S. Wang, and Q. Huang, "Improvement of heat-induced fibril assembly of soy β-conglycinin (7S Globulins) at pH 2.0 through electrostatic screening," *Food Research International*, vol. 46, no. 1, pp. 229–236, 2012.

[5] C. Akkermans, A. J. Van der Goot, P. Venema et al., "Micrometer-sized fibrillar protein aggregates from soy glycinin and soy protein isolate," *Journal of Agricultural and Food Chemistry*, vol. 55, no. 24, pp. 9877–9882, 2007.

[6] L. N. Arnaudov and R. De Vries, "Thermally induced fibrillar aggregation of hen egg white lysozyme," *Biophysical Journal*, vol. 88, no. 1, pp. 515–526, 2005.

[7] E. Linden and P. Venema, "Self-assembly and aggregation of proteins," *Current Opinion in Colloid and Interface Science*, vol. 12, no. 4-5, pp. 158–165, 2007.

[8] Y.-Z. Gao, H.-H. Xu, T.-T. Ju, and X.-H. Zhao, "The effect of limited proteolysis by different proteases on the formation of whey protein fibrils," *Journal of Dairy Science*, vol. 96, no. 12, pp. 7383–7392, 2013.

[9] M. Landreh, M. R. Sawaya, M. S. Hipp, D. S. Eisenberg, K. Wüthrich, and F. U. Hartl, "The formation, function and regulation of amyloids: insights from structural biology," *Journal of Internal Medicine*, vol. 280, no. 2, pp. 164–176, 2016.

[10] J. Mukherjee and M. N. Gupta, "Protein aggregates: forms, functions and applications," *International Journal of Biological Macromolecules*, vol. 97, pp. 778–789, 2016.

[11] C. Akkermans, P. Venema, A. J. van der Goot et al., "Peptides are building blocks of heat-induced fibrillar protein aggregates of β-lactoglobulin formed at pH 2," *Biomacromolecules*, vol. 9, no. 5, pp. 1474–1479, 2008a.

[12] C. Lara, S. Gourdin-Bertin, J. Adamcik, S. Bolisetty, and R. Mezzenga, "Self-assembly of ovalbumin into amyloid and non-amyloid fibrils," *Biomacromolecules*, vol. 13, no. 12, pp. 4213–4221, 2012.

[13] A. Kroes-Nijboer, P. Venema, J. Bouman, and E. van der Linden, "Influence of protein hydrolysis on the growth kinetics of β-lg fibrils," *Langmuir*, vol. 27, no. 10, pp. 5753–5761, 2011.

[14] S. Y. Kim, P. S. W. Park, and K. C. Rhee, "Functional properties of proteolytic enzyme modified soy protein isolate," *Journal of Agricultural and Food Chemistry*, vol. 38, no. 3, pp. 651–656, 1990.

[15] M. Mohammadian and A. Madadlou, "Characterization of fibrillated antioxidant whey protein hydrolysate and comparison with fibrillated protein solution," *Food Hydrocolloids*, vol. 52, pp. 221–230, 2016.

[16] C.-H. Tang, Y.-H. Zhang, Q.-B. Wen, and Q. Huang, "formation of amyloid fibrils from kidney bean 7S globulin (phaseolin) at pH 2.0," *Journal of Agricultural and Food Chemistry*, vol. 58, no. 13, pp. 8061–8068, 2010.

[17] P. M. Nielsen, D. Petersen, and C. Dambmann, "Improved method for determining food protein degree of hydrolysis," *Journal of Food Science*, vol. 66, no. 5, pp. 642–646, 2001.

[18] U. K. Laemmli, "Cleavage of structural proteins during the assembly of the head of bacteriophage T4," *Nature*, vol. 227, no. 5259, pp. 680–685, 1970.

[19] M. Cardamone and N. K. Puri, "Spectrofluorimetric assessment of the surface hydrophobicity of proteins," *Biochemical Journal*, vol. 282, no. 2, pp. 589–593, 1992.

[20] D. Luo, Q. Zhao, M. Zhao et al., "Effects of limited proteolysis and high-pressure homogenisation on structural and functional characteristics of glycinin," *Food Chemistry*, vol. 122, no. 1, pp. 25–30, 2010.

[21] S. M. Loveday, S. G. Anema, and H. &Singh, "β-Lactoglobulin nanofibrils: the long and the short of it," *International Dairy Journal*, vol. 67, pp. 35–45, 2016.

[22] X. D. Sun, "Enzymatic hydrolysis of soy proteins and the hydrolysates utilisation," *International Journal of Food Science & Technology*, vol. 46, no. 12, pp. 2447–2459, 2011.

[23] S. K. Chaturvedi, M. K. Siddiqi, P. Alam, and R. H. Khan, "Protein misfolding and aggregation: mechanism, factors and detection," *Process Biochemistry*, vol. 51, no. 9, pp. 1183–1192, 2016.

[24] M. Anderson, O. V. Bocharova, N. Makarava, L. Breydo, V. V. Salnikov, and I. V. Baskakov, "Polymorphism and ultrastructural organization of prion protein amyloid fibrils: an insight from high resolution atomic force microscopy," *Journal of Molecular Biology*, vol. 358, no. 2, pp. 580–596, 2006.

[25] K. L. De Jong, B. Incledon, C. M. Yip, and M. R. DeFelippis, "Amyloid fibrils of glucagon characterized by high-resolution atomic force microscopy," *Biophysical Journal*, vol. 91, no. 5, pp. 1905–1914, 2006.

[26] K. Makabe, D. Mcelheny, V. Tereshko et al., "Atomic structures of peptide self-assembly mimics," *Proceedings of the National Academy of Sciences*, vol. 103, no. 47, pp. 17753–17758, 2006.

[27] C. Veerman, H. Ruis, L. M. C. Sagis, and E. van der Linden, "Effect of electrostatic interactions on the percolation concentration of fibrillar β-lactoglobulin gelsfibrillar beta-lactoglobulin gels," *Biomacromolecules*, vol. 3, no. 4, pp. 869–873, 2002.

[28] F. Chiti and C. M. Dobson, "Protein misfolding, functional amyloid, and human disease," *Annual Review Of Biochemistry*, vol. 75, no. 1, pp. 333–366, 2006.

[29] C. Akkermans, P. Venema, A. J. van der Goot, R. M. Boom, and E. van der Linden, "Enzyme-induced formation of β-lactoglobulin fibrils by AspN endoproteinase," *Food Biophysics*, vol. 3, no. 4, pp. 390–394, 2008b.

[30] D. Mahl, J. Diendorf, W. Meyer-Zaika, and M. Epple, "Possibilities and limitations of different analytical methods for the size determination of a bimodal dispersion of metallic nanoparticles," *Colloids and Surfaces A: Physicochemical and Engineering Aspects*, vol. 377, no. 1–3, pp. 386–392, 2011.

[31] C. D. Munialo, A. H. Martin, E. van der Linden, and H. H. J. De Jongh, "Fibril formation from pea protein and subsequent gel formation," *Journal of Agricultural and Food Chemistry*, vol. 62, no. 11, pp. 2418–2427, 2014.

[32] J. Xu, B. Qi, Q. Zhao, and H. Jin, "Relationship between structural properties and surface hydrophobicity of soybean protein isolate," *Journal of the Chinese Cereals & Oils Association*, vol. 30, no. 8, pp. 32–36, 2015.

[33] W. Xia, H. Zhang, J. Chen et al., "Formation of amyloid fibrils from soy protein hydrolysate: effects of selective proteolysis on β-conglycinin," *Food Research International*, vol. 100, no. 2, pp. 268–276, 2017.

[34] M. Nilsson, "Techniques to study amyloid fibril formation in vitro," *Methods*, vol. 34, no. 1, pp. 151–160, 2004.

[35] G. Keliényi, "On the histochemistry of azo group-free thiazole dyes," *Journal of Histochemistry & Cytochemistry*, vol. 15, no. 3, pp. 172–180, 1967.

[36] P. S. Vassar and C. F. Culling, "Fluorescent stains, with special reference to amyloid and connective tissues," *Archives of Pathology*, vol. 68, no. 5, p. 487, 1959.

[37] M. Biancalana and S. Koide, "Molecular mechanism of Thioflavin-T binding to amyloid fibrils," *Biochimica et Biophysica Acta (BBA)—Proteins and Proteomics*, vol. 1804, no. 7, pp. 1405–1412, 2010.

[38] M. R. H. Krebs, A. M. Bromley, and A. M. Donald, "The binding of thioflavin-T to amyloid fibrils: localisation and implications," *Journal of Structural Biology*, vol. 149, no. 1, pp. 30–37, 2005.

[39] C. Chothia, "Conformation of twisted β-pleated sheets in proteins," *Journal of Molecular Biology*, vol. 75, no. 2, pp. 295–302, 1973.

[40] M. Biancalana, K. Makabe, A. Koide, and S. Koide, "Aromatic cross-strand ladders control the structure and stability of β-rich peptide self-assembly mimics," *Journal of Molecular Biology*, vol. 383, no. 1, pp. 0–213, 2008.

[41] H. LeVine, "Thioflavine T interaction with amyloid β-sheet structures," *Amyloid*, vol. 2, no. 1, pp. 1–6, 1995.

[42] S. Raimon, I. Lascu, and S. J. Saupe, "On the binding of Thioflavin-T to HET-s amyloid fibrils assembled at pH 2," *Journal of Structural Biology*, vol. 162, no. 3, pp. 387–396, 2008.

[43] Z. Min, H. Shubo, Z. Feimeng, S. A. Carter, and A. L. Fink, "Annular oligomeric amyloid intermediates observed by in situ atomic force microscopy," *Journal of Biological Chemistry*, vol. 279, no. 23, pp. 24452–24459, 2004.

[44] R. Sabate, L. Rodriguez-Santiago, M. S. J., and S. Saupe, "Thioflavin-T excimer formation upon interaction with amyloid fibersfibers," *Chemical Communications*, vol. 49, no. 51, pp. 5745–5747, 2013.

[45] S. G. Sodupe, L. M. C. Sagis, and E. van der Linden, "Effect of stirring and seeding on whey protein fibril formation," *Journal of Agricultural and Food Chemistry*, vol. 55, no. 14, pp. 5661–5669, 2007.

[46] R. Mishra, K. SöRgjerd, M. S. Nyström, A. Nordigården, Y. C. Yu, and P. Hammarström, "Lysozyme amyloidogenesis is accelerated by specific nicking and fragmentation but decelerated by intact protein binding and conversion," *Journal of Molecular Biology*, vol. 366, no. 3, pp. 1040–1044, 2007.

[47] S. Jones and J. M. Thornton, "Analysis of protein-protein interaction sites using surface patches 1 1Edited by G. Von Heijne," *Journal of Molecular Biology*, vol. 272, no. 1, pp. 121–132, 1997.

[48] G. G. Tartaglia, C. Andrea, P. Riccardo, and C. Amedeo, "The role of aromaticity, exposed surface, and dipole moment in determining protein aggregation rates," *Protein Science*, vol. 13, no. 7, pp. 1939–1941, 2010.

[49] A. Kroes-Nijboer, P. Venema, and E. v. d. Linden, "Fibrillar structures in food," *Food & Function*, vol. 3, no. 3, pp. 221–227, 2012.

[50] D. Zhao, L. Li, D. Xu et al., "Application of ultrasound pretreatment and glycation in regulating the heat-induced amyloid-like aggregation of β-lactoglobulin," *Food Hydrocolloids*, vol. 80, pp. 122–129, 2018.

[51] H. Kishimura, Y. Tokuda, M. Yabe, S. Klomklao, S. Benjakul, and S. Ando, "Trypsins from the pyloric ceca of jacopever (Sebastes schlegelii) and elkhorn sculpin (*Alcichthys alcicornis*): isolation and characterization," *Food Chemistry*, vol. 100, no. 4, pp. 1490–1495, 2007.

[52] H. Hu, J. Wu, E. C. Y. Li-Chan et al., "Effects of ultrasound on structural and physical properties of soy protein isolate (SPI) dispersions," *Food Hydrocolloids*, vol. 30, no. 2, pp. 647–65510, 2013.

[53] L. Shen and C.-H. Tang, "Microfluidization as a potential technique to modify surface properties of soy protein isolate," *Food Research International*, vol. 48, no. 1, pp. 108–118, 2012.

[54] A. C. Dave, S. M. Loveday, S. G. Anema et al., "β-Lactoglobulin self-assembly: structural changes in early stages and disulfide bonding in fibrils," *Journal of Agricultural and Food Chemistry*, vol. 61, no. 32, pp. 7817–7828, 2013.

[55] E. Zerovnik, "Amyloid-fibril formation. Proposed mechanisms and relevance to conformational disease," *European Journal of Biochemistry*, vol. 269, no. 269, pp. 3362–3371, 2002.

[56] G. Zandomeneghi, M. Krebs, and M. Mccammon, "FTIR reveals structural differences between native β-sheet proteins and amyloid fibrils," *Protein Science*, vol. 13, no. 12, pp. 3314–3321, 2004.

[57] V. Castelletto, S. Kirkham, I. W. Hamley, M. Kowalczyk, M. Reza, and J. Ruokolainen, "Self-assembly of the toll-like receptor agonist macrophage-activating lipopeptide MALP-2 and of its constituent peptide," *Biomacromolecules*, vol. 17, no. 2, pp. 631–640, 2016.

[58] R. V. Ulijn and A. M. Smith, "ChemInform abstract: designing peptide-based nanomaterials," *Cheminform*, vol. 39, no. 24, pp. 664–675, 2010.

[59] D. T. Seroski and G. A. Hudalla, "Self-assembled peptide and protein nanofibers for biomedical applications," *Biomedical Applications of Functionalized Nanomaterials*, Elsevier, Amsterdam, Netherlands, pp. 569–598, 2018.

[60] J. I. Harris, R. D. Cole, and N. G. Pon, "The kinetics of acid hydrolysis of dipeptides," *Biochemical Journal*, vol. 62, no. 1, pp. 154–159, 1956.

[61] E. Frare, P. Polverino de Laureto, C. M. Dobson, A. Fontana, and A. Fontana, "A highly amyloidogenic region of hen lysozyme," *Journal of Molecular Biology*, vol. 340, no. 5, pp. 1153–1165, 2004.